Analysis of resonant sensors based on mutually injection-locked oscillators beyond the critical Duffing amplitude

Jérôme Juillard, Ali Mostafa, Pietro Maris Ferreira

Analysis of resonant sensors based on mutually injection-locked oscillators beyond the critical Duffing amplitude

Jérôme Juillard, Ali Mostafa, Pietro Maris Ferreira
Mixed-Signals Circuits and Systems (MiSCaS)
GEEPS, UMR8507, CNRS, CentraleSupélec, UPSud, UPMC
Gif-sur-Yvette, France
jerome.juillard@centralesupelec.fr

***Abstract*— Sensor architectures based on coupled resonators are receiving increased interest from the resonant sensing community. Certain output metrics of such sensors have an increased sensitivity to the measurand, compared to conventional resonant sensors with frequency-modulated outputs. In the present paper, we extend our study of the properties of mutually injection-locked oscillators (MILOs) into the nonlinear domain, assuming the resonators are subject to cubic restoring forces. Our analysis shows that, depending on the softening or hardening character of the nonlinearity, some MILOs may be operated well above the critical Duffing amplitude. Moreover, it turns out that all the output metrics of such MILOs are not similarly affected by noise. A typical example is given, in which we show that, above the critical Duffing amplitude, phase difference measurements are limited by the A-f effect, whereas amplitude ratio measurements are not. These theoretical results are supported by transient simulations.**

Keywords—resonant sensors; coupled resonators; MEMS

I. INTRODUCTION

Recent years have seen the development of several sensor architectures based on coupled MEMS resonators, such as open-loop or closed-loop sensors based on mode-localization [1-4] or on mutually-injection locked oscillators (MILOs) [5-6]. So far, our study of coupled architectures has been confined to their operation in the linear regime, below the critical Duffing amplitude which marks the onset of the A-f effect in conventional resonant sensors based on a single resonator (with a cubic nonlinearity) [7]. In this framework, we have shown that the increased sensitivity to the quantity of interest of the output metrics of coupled architectures is always compensated by an increased sensitivity to external fluctuations [8], such as thermomechanical noise [9]. Thus, in the linear regime, there is little to be gained in terms of "ultimate" resolution when two coupled resonators are used instead of a single one.

With the present paper, we show that this conclusion is no longer valid in the nonlinear domain, as far as MILOs are concerned. MILOs consist in two resonators with nominally identical resonance frequencies and quality factors, placed in a nonlinear feedback loop designed so that the resonators oscillate in quadrature. When a stiffness or mass mismatch ε is induced between the resonators (e.g. electrostatically), the resonance frequencies of the resonators are no longer identical. The nonlinear mixer then ensures that the system remains in a phase-locked state, but with a phase difference which deviates from its nominal value. Within a certain measurement range, this deviation then provides a high-sensitivity measurement of the stiffness mismatch between the resonators, and hence of the quantity of interest. Depending on the parameters of the architecture, other output metrics may also be used, such as the ratio of the motional amplitudes of the resonators. It is shown in [10] that operation in the nonlinear regime of such MILOs may result in an increased measurement range, at the cost of a decreased sensitivity.

The theoretical framework of this paper, described in section II, is limited to a MILO consisting of two nominally identical, nonlinearly coupled resonators with cubic stiffness. In section III, we apply perturbation techniques to the governing equations of the system in order to perform sensitivity analysis. We show that the ultimate resolution that can be expected of the phase difference or pulsation output metrics is limited by the A-f effect. This is as opposed to the ultimate resolution of the amplitude ratio output metric, which is improved as the driving force and the oscillation amplitude are increased, even above the critical Duffing amplitude. These theoretical results, based on a quasi-static analysis, are validated by transient simulations. Section IV is dedicated to concluding remarks and perspectives.

II. THEORETICAL FRAMEWORK

We consider the MILO depicted in Fig. 1, which is almost the same as the one studied in [10]. It consists of two resonators with a softening Duffing nonlinearity (characterized by a Duffing coefficient $\gamma < 0$), a nonlinear mixer and a $\pi/4$ phase-shift in both branches. Following the harmonic balance approach of [5], in the absence of external perturbations, the system is governed by a set of 4 (non-dimensionalized) equations

$$\mathbf{g}(\mathbf{s}, \varepsilon) = \mathbf{0}\,, \tag{1}$$

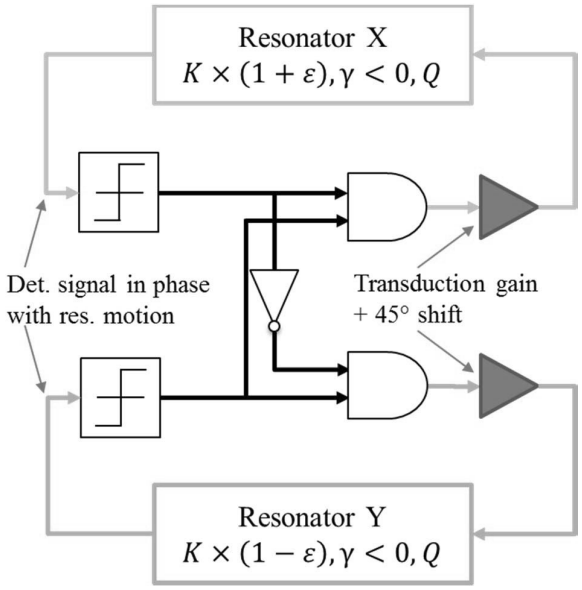

Fig. 1. High-level schematic of a MILO consisting of two nonlinear resonators with a relative stiffness mismatch 2ε, a digital nonlinear mixer and two gain/phase adaptation stages.

where

$$g_1 = \left(1+\varepsilon+\frac{3}{4}\gamma X^2-\omega^2\right)X - \frac{F}{\pi}\left(\cos\frac{\pi}{4}+\cos\left(\frac{\pi}{4}+\phi\right)\right) \quad (2)$$

$$g_2 = \frac{\omega}{Q}X - \frac{F}{\pi}\left(\sin\frac{\pi}{4}+\sin\left(\frac{\pi}{4}+\phi\right)\right) \quad (3)$$

$$g_3 = \left(1-\varepsilon+\frac{3}{4}\gamma Y^2-\omega^2\right)Y - \frac{F}{\pi}\left(\cos\frac{\pi}{4}-\cos\left(\frac{\pi}{4}-\phi\right)\right) \quad (4)$$

$$g_4 = \frac{\omega}{Q}Y - \frac{F}{\pi}\left(\sin\frac{\pi}{4}-\sin\left(\frac{\pi}{4}-\phi\right)\right) = 0 \quad (5)$$

where the state of the system

$$\mathbf{s} = \begin{bmatrix} X & Y & \omega & \phi \end{bmatrix}^T \quad (6)$$

consists in mechanical oscillation amplitudes X and Y, oscillation pulsation ω and phase difference ϕ, where F is the magnitude of the excitation force, Q is the quality factor of the resonators, and ε is a detuning parameter, corresponding to the physical quantity of interest one seeks to measure.

Note that this detuning parameter appears in (2) *and* in (4), with opposite signs, as opposed to [10] for example. Consequently, when $\varepsilon = 0$, the nominal state of the system verifies, as in [10]

$$\phi = \pi/2\,,\ X/Y = 1 \quad (7)$$

but the sensitivity to mismatch of the output metrics is multiplied by 2 compared to the cases studied in our previous studies, and the locking range of the MILO (in terms of mismatch) is also divided by 2.

III. Sensitivity analysis of a nonlinear MILO

A. Definition of a figure of merit

The performance of this architecture as a sensor can be studied with rather simple sensitivity analysis techniques. For example, the sensitivity of the system state $\mathbf{s}$ to ε may be derived from (1) as follows

$$\begin{aligned} &\mathbf{g}(\mathbf{s}+\delta\mathbf{s}, \varepsilon+\delta\varepsilon) = \mathbf{0} \Rightarrow \\ &\mathbf{g}(\mathbf{s}, \varepsilon) + \mathbf{J}_\mathbf{s} \times \delta\mathbf{s} + \begin{bmatrix} X & 0 & -Y & 0 \end{bmatrix}^T \delta\varepsilon \approx 0 \Rightarrow, \\ &\delta\mathbf{s} \approx -\mathbf{J}_\mathbf{s}^{-1} \times \begin{bmatrix} X & 0 & -Y & 0 \end{bmatrix}^T \delta\varepsilon \end{aligned} \quad (8)$$

where $\mathbf{J}_\mathbf{s}$ is the jacobian of $\mathbf{g}$ with respect to state $\mathbf{s}$. The sensitivity of any output metric $M(\mathbf{s})$ to ε can then be derived from (8) as

$$\frac{dM}{d\varepsilon} = -\frac{dM}{d\mathbf{s}} \times \mathbf{J}_\mathbf{s}^{-1} \times \begin{bmatrix} X & 0 & -Y & 0 \end{bmatrix}^T. \quad (9)$$

The sensitivity of $M(\mathbf{s})$ to other sorts of fluctuations may be established in a similar manner. In the case of thermomechanical fluctuations, which is of interest in order to determine the "ultimate" performance attainable with a given output metric, one must consider the perturbed system:

$$\mathbf{g}(\mathbf{s}+\delta\mathbf{s}, \varepsilon) = \mathbf{n} \quad (10)$$

where the components of $\mathbf{n}$ are independent, slowly-fluctuating "forces", with equal magnitudes. The sensitivity of $M(\mathbf{s})$ to these random fluctuations can be defined as the RMS value of the sensitivities to the independent noise components, i.e.

$$\frac{dM}{dn} = \sqrt{\sum_{i=1}^{4}\left(\frac{dM}{dn_i}\right)^2}. \quad (11)$$

A first-order expansion of (10) yields:

$$\delta\mathbf{s} \approx \mathbf{J}_\mathbf{s}^{-1} \times \mathbf{n}\,, \quad (12)$$

From (11) and (12), it follows that the sensitivity of $M(\mathbf{s})$ to random fluctuations is:

$$\frac{dM}{dn} = \left\| \frac{dM}{d\mathbf{s}} \times \mathbf{J}_\mathbf{s}^{-1} \right\|_2. \quad (13)$$

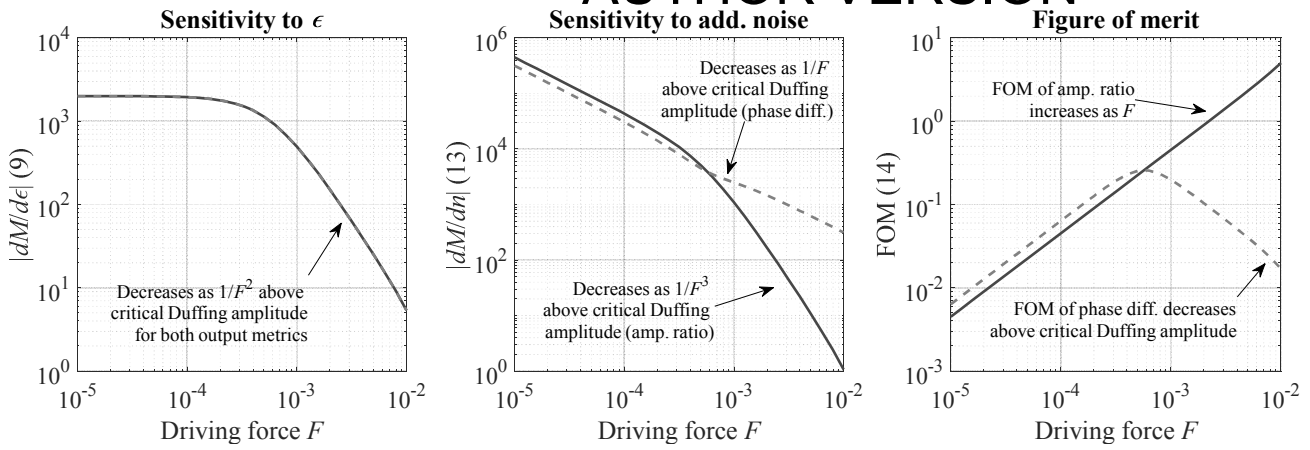

Fig. 2. Performance of amplitude ratio (solid blue line) and of phase difference (dashed red line) output metrics at ϵ=0 vs. driving force, for Q=10^3 and γ=-10^{-2}: sensitivity to ϵ (left), sensitivity to additive noise (center), and figure of merit (right).

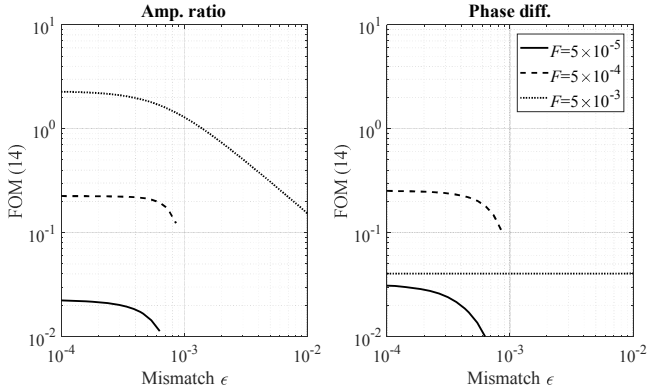

Fig. 3. Figure of merit of the amplitude ratio (left) and phase difference (right) output metrics vs. ϵ, for different values of the driving force, other system parameters as in Fig. 2.

Equations (9) and (13) may be used to define a figure of merit for $M(\mathbf{s})$, as the ratio of the sensitivity to ε to the sensitivity to noise, i.e. :

$$\mathrm{FOM}(M)=\frac{|dM/d\varepsilon|}{dM/dn} \tag{14}$$

which should be maximized in order to improve sensor performance, i.e. sensitivity to ε and immunity from noise.

B. Comparison of different output metrics

In the linear regime, close to $\varepsilon=0$ we find that

$$\mathrm{FOM}(\phi)=2\times\frac{QF}{\pi}=\sqrt{2}\times\mathrm{FOM}\left(\frac{X}{Y}\right), \tag{15}$$

so that, for the considered architecture phase difference is a slightly better output metric than amplitude ratio, although both have the same sensitivity to ε [10]. The figure of merit increases linearly with the amplitude of the drive, as can be expected [5,8], until the critical Duffing amplitude is neared.

Above the critical Duffing amplitude, the situation is almost dramatically different: while the figure of merit of the amplitude ratio output metric keeps increasing with the drive amplitude, that of the phase difference starts decreasing, a signature of the A-f effect (or A-ϕ in the present case). This is illustrated in Fig. 2.

More accurately, above the critical Duffing amplitude, the sensitivity to ε of both output metrics starts dropping as F^{-2}. From (13), one may show that the sensitivity to noise of the phase difference output metric decreases as F^{-1} in the nonlinear regime (as in the linear regime, in fact). Thus, the figure of merit for ϕ decreases as F^{-1}. On the other hand, the sensitivity to noise of the amplitude ratio output metric decreases as F^{-3} in the nonlinear regime (as opposed to F^{-1} in the linear regime). Thus, the figure of merit for the amplitude ratio keeps increasing proportionally to F, as it does below the critical Duffing amplitude. In fact, we have

$$\mathrm{FOM}\left(\frac{X}{Y}\right)\approx\sqrt{2}\times\frac{QF}{\pi} \tag{16}$$

regardless of the operating regime, as shown in Fig. 2.

It is worth noting that this remarkable property of the amplitude ratio output metric is valid only in a reduced range around $\varepsilon=0$, in spite of the nonlinear enhancement of the locking range of the MILO [10]. Although no closed-form formula has been derived for the range of validity of (16), our calculations suggest that this result holds only within the *linear* locking range of the architecture, as Fig. 3 indicates.

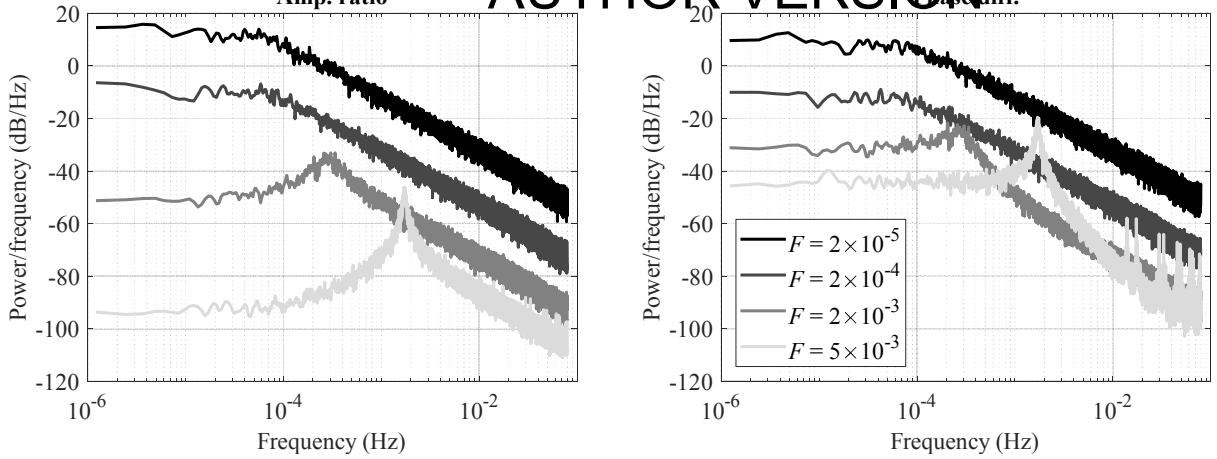

Fig. 4. Noise spectra obtained by transient simulation for the amplitude ratio (left) and phase difference (right) output metrics, with ε=0, Q=10^3 and γ=-10^{-2} and different values of the driving force.

C. *Transient simulation*

These theoretical results, based on a quasi-static analysis, are validated by transient simulations, with Simulink, of a MILO with parameters $Q = 10^3$, $\gamma = -10^{-2}$ and $\varepsilon = 0$. Independent white noise sources are placed at the inputs of the resonators to simulate the effect of thermomechanical forces. Four values of driving force are simulated: $F = 2\times10^{-5}$, $F = 2\times10^{-4}$, $F = 2\times10^{-3}$, $F = 5\times10^{-3}$, with the noise power kept constant. The power spectrum of the amplitude ratio and phase difference fluctuations are plotted in Fig. 4.

These simulated results are in very good agreement with our theory, which predicts that, in the last three simulations, the near-DC power of the phase difference should be 21dB, 41dB and 54dB below that of the linear case ($F = 2\times10^{-5}$), whereas that of the amplitude ratio should be 21dB, 62dB and 106dB below the linear case.

It is also worth noting that a resonance peak appears at the cutoff frequency of the system at large driving forces. A quantitative analysis of this phenomenon would require a more involved dynamic perturbation analysis, as in [5].

IV. CONCLUSION

We have presented in this paper a theoretical analysis of the properties of a MILO-based architecture, when the resonators are pushed into the nonlinear regime. A general figure of merit for the different output metrics used in coupled architectures was proposed. In the case of the framework defined in section II, it was shown that this figure of merit increases monotonically with drive amplitude, whether below or above the critical Duffing amplitude, when the amplitude ratio is used as an output metric. On the other hand, phase difference does not perform as well in the nonlinear regime, its figure of merit decreasing with the drive amplitude once the A-f effect kicks in.

It should be stressed that this result can be extended to other frameworks than the one considered in this paper. For example, in the case of hardening nonlinearities, a similar result is found if the phase-shift of the MILO is chosen to be $3\pi/4$ instead of $\pi/4$. More generally, similar results hold provided the amplitude ratio is an output metric at all, i.e. provided its sensitivity to ε is non-zero. One should also note that a similar qualitative behavior of the output metrics is also observed when the resonators are not perfectly matched (in terms of Duffing coefficient, quality factor or driving force), even by a large margin. Finally, another point of interest is that (16) is independent of the value of γ: although this calls for a formal proof, this suggests that (16) may be valid for other types of static nonlinearities (e.g. non-polynomial).

Although such results seem to open the way for interesting new paradigms of resonant sensors, whose performance are not limited by nonlinear phenomena, one should also consider their practical limitations. First of all, the amplitude ratio is an analog quantity, as opposed to frequency or phase-difference: thus a sensor using amplitude ratio as an output metric will require analog-to-digital conversion (ADC) stages, with an added cost in terms of surface and power consumption compared to quasi-digital solutions. Moreover, the requirements on the ADC stage(s) are likely to become more stringent as the amplitude increases, because of the reduced sensitivity of such MILOs in the nonlinear regime [10]. In this respect, advantageous design tradeoffs can probably be scavenged from the field of (amplitude modulated) mode-matched gyroscopes [11-12], with which MILOs share many common points. Finally, note that our results are significant only for sensors that are limited by additive noise at the input of the resonator [7,9] and do not apply in the case of random parametric fluctuations, such as stiffness fluctuations [13].

Our continuing work on this subject is dedicated to generalizing our formal approach to other architectures and other nonlinearities (e.g. damping, excitation and detection), deriving optimal output metrics, and obtaining an experimental validation of our results.

REFERENCES

[1] C. Zhao et al., "A review on coupled MEMS resonators for sensing applications utilizing mode localization," Sensors and Actuators A: Physical, vol. 249, pp. 93-111, 2016.

[2] P. Thiruvenkatanathan, J. Yan and A. A. Seshia, "Differential amplification of structural perturbations in weakly coupled MEMS resonators," IEEE Transactions on Ultrasonics, Ferroelectrics 9and Frequency Control, vol. 57, pp. 690-697, 2010.

[3] C. Zhao et al., "A closed-loop readout configuration for mode-localized resonant MEMS sensors" IEEE Journal of Microelectromechanical Systems, vol. 26, pp. 501-503, 2017.

[4] C. Zhao et al. "Experimental Observation of Noise Reduction in Weakly Coupled Nonlinear MEMS Resonators", IEEE Journal of Microelectromechanical Systems, vol. 26, pp. 1196-1203, 2017.

[5] J. Juillard, P. Prache and N. Barniol, "Analysis of mutually injection-locked oscillators for differential resonant sensing," IEEE Transactions on Circuits and Systems I: Regular Papers, vol. 63, pp. 1055-1066, 2016.

[6] P. Prache, et al., "Design and characterization of a monolithic CMOS-MEMS mutually injection-locked oscillator for differential resonant sensing", Sensors and Actuators A: Physical, vol. 269, pp. 160-170, 2017.

[7] D. K. Agrawal, A. A. Seshia, "An analytical formulation for phase noise in MEMS oscillators", IEEE Transactions on Ultrasonics, Ferroelectrics and Frequency Control, vol. 61, pp. 1938-1952, 2014.

[8] J. Juillard, P. Prache, P.M. Ferreira, N. Barniol, "Ultimate limits of differential resonant MEMS sensors based on two coupled resonators", IEEE Transactions on Ultrasonics, Ferroelectrics and Frequency Control, 2018 (accepted).

[9] A. N. Cleland, M. L. Roukes, "Noise processes in nanomechanical resonators", Journal of Applied Physics, vol. 92, pp. 2758-2769, 2002.

[10] J. Juillard, A. Mostafa, P. M. Ferreira, "Nonlinear enhancement of locking range of mutually injection-locked oscillators for resonant sensing applications", European Frequency and Time Forum, 2018 (accepted).

[11] I. Prikhodko et al. "Mode-matched MEMS Coriolis vibratory gyroscopes: myth or reality?", IEEE/ION Position, Location and Navigation Symposium (PLANS), 4 pp., 2016.

[12] M. F. Zaman, A. Sharma, F. Ayazi, "High performance matched-mode tuning fork gyroscope", IEEE International Conference on MEMS, pp. 66-69, 2006.

[13] M. Sansa, et al. "Frequency fluctuations in silicon nanoresonators", Nature Nanotechnology, vol. 11, pp. 552-558, 2016.